FRACTURES IN ENCELADUS' LITHOSPHERE: CONSTRAINTS FROM 3D FINITE ELEMENT MODELING. Mallory J. Kinczyk[1], Paul K. Byrne[1], Kate L. Craft[2], DelWayne R. Bohnenstiehl[1]. [1]Department of Marine, Earth, and Atmospheric Sciences, North Carolina State University, Raleigh, NC 27695, [2]The Johns Hopkins University Applied Physics Laboratory, Laurel, MD 20723.

Introduction: Enceladus remains one of the most enigmatic icy satellites in the Solar System. Boasting the highly active South Polar Terrain with its plume material [1], its ancient, cratered terrain, and the expansive young surfaces that display only a minimal record of impact cratering, Enceladus is unusually active for such a small world (r = 252 km), and a prime astrobiological target. Although it is exciting to think about the prospects of sending a probe to explore subsurface water at Enceladus [2], it is critical to have a robust understanding of the nature of the ice shell before moving towards interior exploration.

One important component is the mechanical behavior of the ice shell. Numerous estimates of the thickness of the ice shell from gravity, topography, and libration [3] exist, but methods incorporating observed surface geology remain sparse [4,5]. More specifically, the behavior of the ice shell is linked to the strength of the lithosphere (or the upper portion of the shell that behaves in a brittle fashion) and the location of the transition from brittle deformation to plastic flow [6], termed the "brittle–ductile transition" or (BDT). Here we use a 3D finite element model to gain insight into the relationship between crater size, lithospheric thickness, and fracture strike reorientation with a goal of approximating the thickness of the brittle portion of the ice shell in the cratered terrain. This parameter will help refine our understanding of how Enceladus' ice shell deforms.

Objective: While there have been numerous studies that have placed estimates on the overall ice shell thickness [3], only a few [e.g., 4,5] have sought to determine the relative contributions of the brittle and ductile regimes to this overall estimate. In previous work, we proposed [7] a potential relationship between the presence of crater–fracture interactions in Enceladus' cratered terrain and lithospheric thickness. This earlier work proposed that under certain conditions at Enceladus, craters act as stress concentrations [9] resulting in many instances of changes in fracture strike with proximity to craters, a style of deformation rarely observed on other icy moons [10]. Spatial analysis [9] indicates that even though there are some craters where fracture reorientation is statistically significant, most are also proximal to other large craters and fracture systems, making the results inconclusive. By developing a numerical model, we can consider a single crater in isolation to better understand the potential factors that influence the interaction between craters and fracture reorientation.

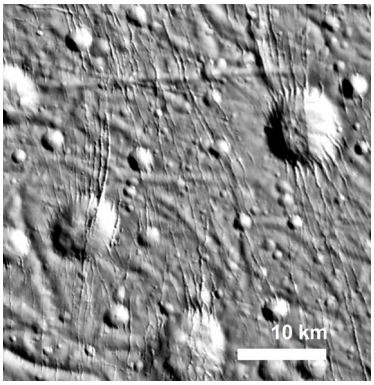

Figure 1. Cratered terrain centered at 5°N, 165°E. Image is from the global mosaic [8]. The fracture network trending N–S shows both straight and deflected segments. Fractures near the three prominent large craters show evidence of strike deflection.

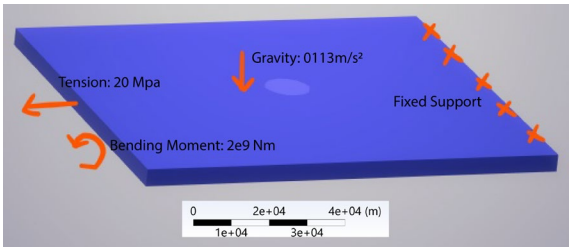

Figure 2. Model boundary conditions including Enceladus' surface gravity, distributed tensile stress, fixed support, and bending moment. Note crater lies at center.

Methods: We use ANSYS, an engineering simulation software, to develop a structural finite element model of Enceladus' brittle lithosphere. **Figure 2** shows our boundary conditions and model setup. The model setup is similar to an example from ref. [11] of a plate fixed at one end with an added bending moment applied to the free end. We then add a general tensile force to promote fracture growth. The bending moment is used to simulate ice shell thickening [3,12], with greater tensile stress at the surface and less at the base of the shell. Tensile stress and bending moment values were chosen based on an average established tensile strength of ice (1.5 MPa) [13] to encourage ice failure. Model iterations vary lithospheric thickness (T_e) at 5 or 10 km thickness, crater diameter (D) at 5 or 10 km, and fracture initiation distance from crater rim perpendicular to the maximum tensile stress direction. Model results of interest are those focused proximal to the crater (2–3 crater radii), ignoring far-field effects.

Results: We find that fracture deflection (example shown in **Figure 3**)—that is, change in strike—is successful under the model conditions and resembles the fracture deflection observed in images of Enceladus'

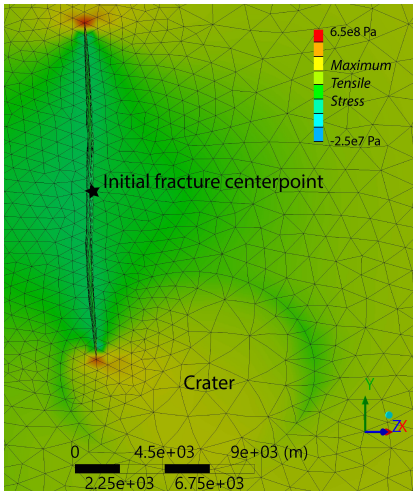

Figure 3. Model result for fracture propagation proximal to a 10 km-diameter crater in a 5 km-thick brittle ice layer. Initial fracture length was 4 km and extended 6.5 km. The fracture strike reorients within ~2 km of the crater rim, trending toward the crater.

cratered terrain (**Figure 1**). **Figure 3** clearly displays the asymmetrical nature of the stress concentration at the crack tip closest to the crater (compared with the symmetrical stress concentration at the opposing crack tip). We also find that deflection decreases with increasing initial distance from the crater. This finding has implications for the nature of fracture formation on Enceladus in this region, indicating that there may, indeed, be a crater-centric formation mechanism. Further, when comparing the results based on lithospheric thickness (**Figure 4**), more relative fracture deflection occurs in the presence of a large crater in a thin lithosphere than most other model scenarios. This latter finding is consistent with observations [7,10] of

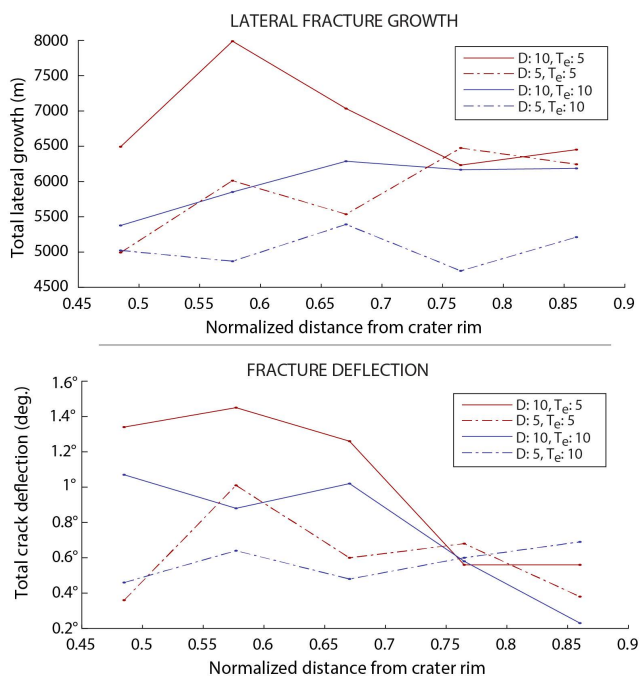

Figure 4. (Top) Plot of lateral crack growth (or lengthening) as a function of normalized initial crack centerpoint distance from crater rim. (Bottom) Plot of crack deflection as a function of normalized initial crack centerpoint distance from crater rim.

large craters influencing fracture strikes more so than small craters. However, the full extent to which crater size and lithospheric thickness influence total fracture deflection is not yet clear.

Our preliminary models incorporated pure tensile stress with no bending moment. Although fractures did propagate, we observed that, with this setup, fractures became arrested before reaching the crater at most initial distances (and became arrested after an arbitrary amount of extension in models without a crater present). These results do not match what we would expect under extreme tensile loads. However, we chose to ignore this condition since our main objective is to forward model crack *deflection* and our applied loads are much lower than would be necessary to cause extreme deformation.

Future Work: The model results presented here are a promising indicator that crater–fracture interactions on Enceladus may depend, at least in part, on lithospheric thickness. However, additional parameters may also play important roles in governing the nature of extensional deformation of the moon's ice shell. Increasing the complexity of these models will help us better identify what key factors are at play, such as:

1. *Lower ductile layer:* It is currently unclear to what extent the presence of a ductile layer within the ice shell influences the distribution of stresses at the surface.
2. *Enceladus' radius of curvature:* Membrane stresses may play an important role in the resulting deformation of the ice shell due to Enceladus' high degree of curvature [3,14]. Incorporating the shell curvature in 3D space with the applied bending moment described above would more accurately replicate the distribution of stresses within the shell.
3. *Multiple fractures:* Fault growth by segment linkage is a well-studied topic on Earth [15]. Due to the en echelon distributions and scalloped nature of many fractures on Enceladus, it is likely that this linkage process has occurred and should be taken into account when modeling fracture development and propagation [16].

References: [1] Porco, C.C. et al. (2006), Science, 311, 1393–1401. [2] Konstantinidis, K. et al. (2016), Acta Astr., 106, 63–89. [3] Hemingway, D., et al. (2018), Enceladus & Icy Moons of Sat., pp. 57–77. [4] Bland, M.T., et al. (2007), Icarus, 192, 92–105. [5] Giese, B., et al. (2008), GRL, 35, 1–5. [6] Kohlstedt, D.L., et al. (1995), JGR, 100, 17587-17602. [7] Kinczyk, M.J., et al. (2018), LPS, 50, 1446. [8] Bland, M.T., et al. (2018), Earth & Spac. Sci., 5, 604–621. [9] Pilkey, W.D. (2008) Peterson's Stress Conc. Fact., 3–6, [10] Martin et al. (2011) LPS, 42, Abstract #2666. [11] Turcotte, D.L. & Schubert, G. (2014), Geodynamics, 3rd Ed., pg. 142. [12] Čadek, et al. (2017), 291, 31–35. [13] Petrovic, J.J. (2003), J. Mat. Sci., 38, 1–6. [14] Turcotte, D.L., et al. (1981), JGR, 86, 3951-3959. [15] Trudgill, B. & Cartwright, J. (1994) Geol. Soc. Am. Bull. 106, 1143–1157 [16] Nahm, A.L. & Kattenhorn, S.A. (2015), Icarus, 258, 67–81.